Simulation Study of Ignition and Burn Characteristics of Fast Ignition DT Targets

Tomoyuki JOHZAKI, Kunioki MIMA and Yasuyuki NAKAO[1)]

Institute of Laser Engineering, Osaka University, 2-6 Yamada-oka, Suita 565-0871, Japan
[1)]*Department of Applied Quantum Physics and Nuclear Engineering, Kyushu University, 744 Motooka, Fukuoka 819-0395, Japan*

(Received 17 April 2007 / Accepted 6 July 2007)

The ignition and burn properties of fast ignition DT targets are evaluated for various-sized core (ignition experiment ~ high gain) on the basis of two-dimensional (2D) burn simulations. A core size of $\rho R \geq 2.0\,\mathrm{g/cm^2}$ is required to achieve explosive burning and then high gain. When the core size is smaller, the target gain drops sharply as core size decreases. Assuming the energy coupling efficiencies from laser to core of 5 % for implosion and 30 % for heating, a target gain of ~170 is obtained with a 1 MJ implosion laser and a 70 kJ heating laser, under optimum heating conditions (10 ps duration, 15 μm spot radius, and $1.0\,\mathrm{g/cm^2}$ heating depth). This requires a very high intensity heating laser ($\sim 1 \times 10^{21}\,\mathrm{W/cm^2}$). In accordance with a scaling for temperature of fast electrons generated by long-duration intense lasers, such a intense laser will generate fast electrons having suitable stopping range for efficient core heating. The sensitivities of ignition condition and gain performance to heating conditions, and the influence of high-Z ions contained in a foam layer on ignition and gain performance are also discussed.

© *2007 The Japan Society of Plasma Science and Nuclear Fusion Research*

Keywords: fast ignition, 2D burn simulation, ignition requirement, gain curve, heating pulse dependence, foam influence

DOI: 10.1585/pfr.2.041

1. Introduction

In fast ignition (FI) scheme [1], where an ultra-intense short-pulse laser rapidly heats an imploded core up to ignition temperature, high gain is expected with small driver energy, compared with conventional central spark ignition scheme.

For FI scheme, Atzeni [2] evaluated the ignition condition on the basis of two-dimensional (2D) simulations for precompressed DT cores and obtained scaling laws for the ignition energy, power, and intensity. However, the compressed core size was assumed to be significantly larger than the size of heating region. In addition, the gain performance was evaluated using the above ignition conditions and a simple formula for burn-up ratio [2, 3]. Application of those scaling laws, therefore, might be limited to such large targets.

At Institute of Laser Engineering (ILE), Osaka University, high energy coupling efficiency from the heating laser to the imploded core and resultant core temperatures of ~1 keV were achieved using the cone guide targets in the Gekko XII–petawatt laser experiments [4]. As the next step, 10 kJ/10 ps Laser for Fusion Experiment (LFEX) for Fast Ignition Realization EXperiment phase-I (FIREX-I) is under construction [5]. A conceptual design of a laser fusion reactor based on FI, "KOYO-FAST" [6], has also been investigated. The compressed core size in FIREX-I will be smaller than the MeV-electron range. The burn property of a small core expected in FIREX-I is different from that of a large-sized high-gain core. To understand the potential of FI and to make the research road map to approach fusion reactor, it is necessary to evaluate the ignition requirements and gain performance for targets of sizes ranging from small (experimental class) to sufficiently large (high gain class).

Previously, we evaluated target gains for various sizes of compressed DT cores (core density of $\rho = 300\,\mathrm{g/cm^3}$ and an isentrope parameter of $\alpha = 2$) on the basis of parametric 2D burn simulations [7]. An evaluation for $\alpha = 3$ was also done. In the present paper, we show the ignition and burn dynamics of FI targets from ignition-experiment-grade cores to high-gain cores. In Sec. 2, we briefly describe the model of 2D burn simulation code "FIBMET" (Fusion Ignition and Burn code with Multiple Energy Transport) and the simulation setup. Section 3 describes the simulation results. Sections 3.1-3.2 discuss the core-size dependences of ignition and burn performances and compare the results with previous studies. Section 3.3 evaluates the heating pulse parameter dependences for a high-gain target. The influence of foam material is evaluated in Sec. 3.4. Section 4 presents the conclusion.

author's e-mail: tjohzaki@ile.osaka-u.ac.jp

© 2007 The Japan Society of Plasma Science and Nuclear Fusion Research

2. Model Description

2.1 Simulation code FIBMET

The Simulation code FIBMET [7] is based on 1-fluid 2-temperature Eulerian hydrodynamic code, written in 2D cylindrical coordinates (r, z) with axial symmetry. In this code, the Thomas-Fermi and ideal gas models are employed for the electron and the ion equations of state, respectively. The energy conservation equation considers electron thermal conduction, radiation effect, fusion-product heating, and external fast electron heating. Electron conduction is treated by the flux-limited Spitzer–Harm's diffusion model. Radiation effect is evaluated by a 1-group flux-limited diffusion model. The radiation interactions considered here are the bremsstrahlung, the inverse-bremsstrahlung and the Thomson scattering. As for fusion reactions, D-T, D-D (two branches) and D-^{3}He reactions are considered. The energy transport of 3.52 MeV alpha-particle is calculated by a multi-group, naturally flux-limited diffusion model [8, 9]. The production rates of other charged particles are much smaller than that of the DT alpha-particle; therefore, these particles are treated by a simple local/instantaneous deposition model. Neutron heating is not essential in DT fuel burning [10], and is neglected here. The FIBMET adopts two methods for dealing with fast electron heating. One is a simple model, adopted by Atzeni [2] and Slutz [11], where the core heating rate is numerically given and added to the energy equation for bulk electrons. The other, more accurate, method treats fast electron transport in the core with a 2D relativistic Fokker–Planck (RFP) code [12, 13]. For the parametric study, however, the 2D RFP part is too expensive, because it requires 5D calculations (2D in real space and 3D in momentum space). Therefore, we adopt the simple heating model.

2.2 Simulation setup

Although implosion dynamics and dense core formation are important issues, especially for cone-guided targets [4], they are not discussed in the present study. At the beginning of the simulation, uniformly-compressed stationary DT plasma spheres are assumed as imploded core profiles. In setting the initial core profiles, we assumed 5 % energy coupling efficiency (η_i) from implosion laser energy ($E_{L,i}$) to the core internal energy (E_{int}), and also assumed a density of $\rho = 300\,\mathrm{g/cm^3}$ and isentrope parameter (the ratio of the fuel pressure to the Fermi pressure) of $\alpha = 2$ (or 3). The value of E_{int} is evaluated by $(4\pi/3)R^3\alpha(3/5)n_e\varepsilon_F$, where R, n_e, and ε_F are the radius, the electron-number density, and the Fermi energy of the compressed core, respectively. For a given $E_{L,i}$ and η_i, the core size becomes smaller as α increases. The simulations were performed for several cores with different sizes (ignition experiment ~ high gain) listed in Table 1.

The core heating process is also crucial. The clarifications of the detailed physics of fast electron generation by ultra-intense laser and its energy transport into the dense cores will lead to the optimization of core heating processes and determination of core heating efficiency. On the other hand, simulations using the simple heating model are important for the evaluation of ignition and burn dynamics, and determining the requirements for ignition and high gain in FI. For core heating, therefore, we simply assumed uniform heating rates [W/kg] for bulk electrons within the cylindrical region (the spot radius r_h [μm] and the optical depth $\rho L_h = \int_0^{L_h} \rho dz$ [g/cm^2]) at the edge of the compressed core, with a duration of τ_h [ps]. The core profile and the heating region are illustrated in Fig. 1.

Table 1 Implosion laser energies and the corresponding compressed core sizes.

Core Type	Implosion Laser $E_{L,i}$ [kJ] (η_i= 5%)	ρR[g/cm^2]	
		$\alpha = 2$	$\alpha = 3$
S1 *1	10	0.69	0.61
S2	25	0.97	0.85
S3 *1	50	1.23	1.07
D1 *2	160	1.59	1.38
H1 *3	560	2.64	2.31
H2 *3	960	3.33	2.91

*1 S1 and S3 correspond to FIREX-I and -II class cores.
*2 D1 corresponds to fusion-burn demo class.
*3 H1 and H2 correspond to high gain cores.

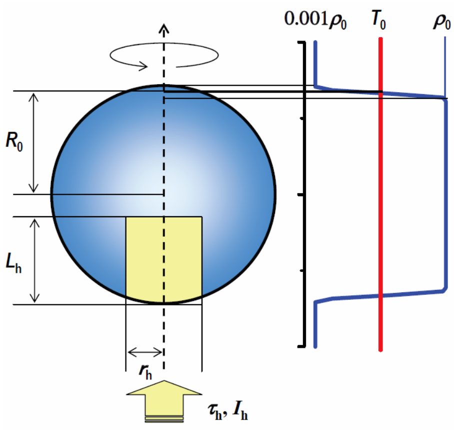

Fig. 1 Schematic view of core profile at the beginning of simulations, and the heating region.

3. Results and Discussion

3.1 Core-Size dependence of ignition and burn performance

First, we show the core-size dependence of ignition and burn properties. Figure 2 shows the temporal profiles of fusion power from S1, S3, and H1 cores. The size of the heating region, r_h and ρL_h are fixed at 15 μm and 1 g/cm^2—almost the same as a sphere with a radius of 3.52 MeV alpha-particle range. The pulse duration is fixed at τ_h = 10 ps. These are close to the optimum values to minimize the ignition energy [2]. The heating pulse intensities I_L [W/cm^2] (the corresponding heating energies E_h [kJ]) are 1.0, 2.6, and 2.6 × 10^{20} W/cm^2 (7.1, 18.4, and 18.4 kJ) for S1, S3, and H1 cores.

The size of the S1 core (0.7 g/cm^2) is comparable to the heating region assumed here. The bulk ion is heated through electro–ion temperature relaxation during the heating pulse injection, and its temperature rises continuously up to about 10 keV. After external heating, however, the core density and temperature decrease rapidly due to expansion since the surrounding cold region confining the heated region does not exist. Thus, fusion output power begins decreasing. For such small targets, explosive burning is never expected. In this case, the tritium burn-up rate (B_T) of 0.64 % was obtained. This feature is so-called "driven ignition" [14] and expected in FIREX-I.

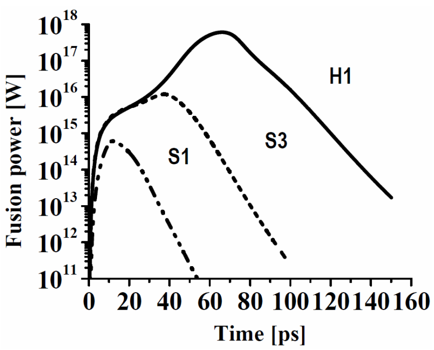

Fig. 2 Fusion output power as a function of time from S1, S3, and H1 cores. The heating energies for each core are 7.1, 18.4, and 18.4 kJ, respectively. The heating pulse duration is 10 ps.

In the case of the S3 core, the core size (1.2 g/cm^2) is larger than the external heating region, and then cold fuel surrounds the heating region. If the heating energy is sufficiently large, alpha-particle self-heating causes the core temperature to increase even after the external heating stops. The burn wave then propagates into the cold region as a deflagration wave, which sustains an increase in fusion output power. The core size is, however, not sufficiently large to achieve explosive fusion burn. The resulting B_T is 4.7 %. This burn property is so-called self-ignition [14] and expected in FIREX-II.

As the core size increases, the volume of the cold region becomes large. The temporal evolutions of fusion burning for the H1 core (ρR = 2.6 g/cm^2) are shown in Fig. 3. The ion is heated above 10 keV with a 10 ps heating pulse. Then, alpha-particle self-heating causes the ion temperature in the heating region to increase continuously. The surrounding region is also heated by alpha-particles and electron thermal conduction, gradually spreading the ignited region. At the same time, the shock wave is driven by the steep pressure gradient between the heating region and the surrounding cold region. Through this period (∼30 ps) after external heating, the burn wave transforms from a deflagration wave to a detonation wave driven by a shock heating. Thus, explosive burning is achieved, and a high burn-up ratio (B_T = 27 %) is obtained.

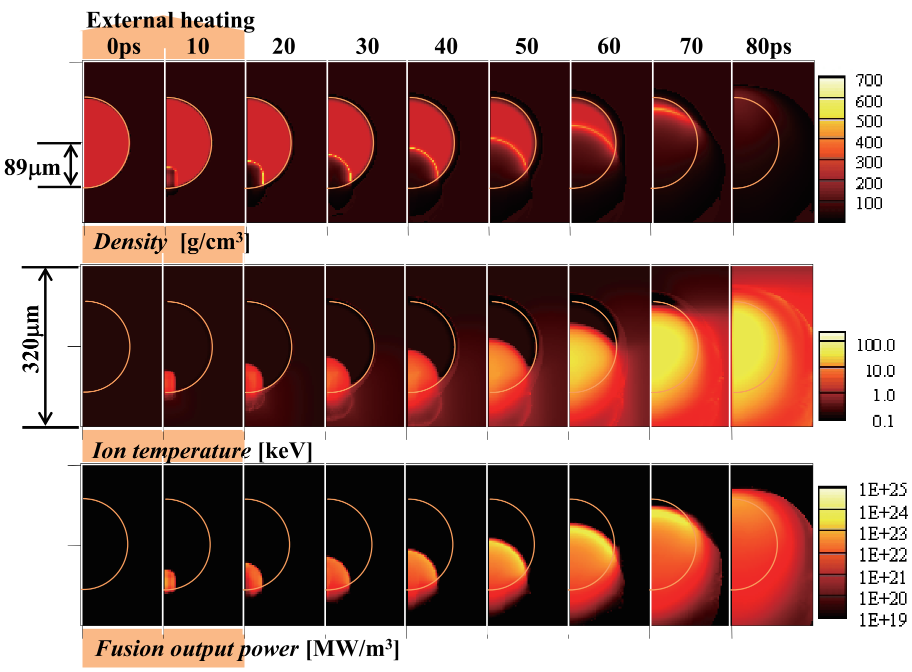

Fig. 3 Temporal evolution of fusion burning, obtained for an H1 core (ρR = 2.6 g/cm^2) with a heating pulse of I_h = 2.6 × 10^{20} W/cm^2, τ_h = 10 ps, r_h = 15 μm and E_h = 18 kJ.

3.2 Gain curve

As shown in the previous section, the burn properties depend on the core size. For further evaluation, we performed simulations for six cores with different sizes with $\alpha = 2$ and 3 (listed in Table 1), by varying the heating pulse energy. Here, the values of r_h, ρL_h, and τ_h are fixed as 15 μm, 1 g/cm^2, and 10 ps, and I_h was varied to maximize the target gain Q for each core. The target gain Q is defined as $Q = E_F/(E_{L,i} + E_{L,h})$, where E_F and $E_{L,h}$ are the fusion output energy and the heating laser energy, respectively. To estimate the target gain, energy coupling efficiencies from laser to core were assumed as $\eta_i = 5\,\%$ for implosion, and $\eta_h = 30\,\%$ for the following core heating. (Such high coupling in core heating is expected in cone-guided targets [4].)

Figure 4 shows plots of the heating energy required to achieve the maximum gain Q_{max} for each target, the maximum gain Q_{max} obtained, and the corresponding burn-up ratio B_T as a function of core size. The heating laser energy $E_{L,h}$ ($\eta_h = 30\,\%$) is also shown on the right axis in Fig. 4 (a). The points from right to left correspond to the results obtained from the H2 core to the S1 core. A core size of $\rho R > 2$ g/cm^2 and $E_h > 20$ kJ ($E_{L,h} > 60$ kJ) are required for high gain. Because the compressed core temperature decreases for a fixed density, the ignition laser energy is slightly enhanced as α decreases. For evaluation of B_T, a simple formula,

$$B_T = \frac{\rho R}{H_B + \rho R}, \tag{1}$$

is widely used, where $H_B = 7$ g/cm^2. In their gain estimation for FI targets, Atzeni [2] and Tabak *et al.* [3] used this formula in their gain estimation. To check the validation of applying this formula to FI, Atzeni *et al.* [15] performed burn simulations, and found that the ignition threshold is $\rho R = 1 - 1.5$ g/cm^2. We obtained similar results. When $\rho R > 2.0$ g/cm^2, Eq. (1) agrees well with the B_T obtained from detailed simulations. B_T depends only on ρR, not on α.

In Fig. 5, Q_{max} is plotted as a function of total laser energy, $E_{L,tot} = E_{L,i} + E_{L,h}$. The open circles correspond to Q_{max} obtained for each core, except for the lowest gain points. The lowest gain point for each α value was obtained from the S1 core, by assuming $E_{L,h} = 10$ kJ which is the FIREX-I heating laser energy. In accordance with the burn properties described in Sec. 3.1, the region of $E_{L,tot} < 40$ kJ is the driven ignition region, where external heating is dominant, and $Q < 1$. The region of 40 kJ $< E_{L,tot} <$ 200 kJ is the self-ignition region where the self-heating of alpha-particles is effective, and $Q = 1 \sim$ a few tens. High gain is achieved with $E_{L,tot} > 200$ kJ. For $\alpha = 2$, a target gain of $Q_{max} = 175$ is obtained with $E_{L,tot} \sim 1$ MJ. In conventional central hot spark ignition, a laser energy of a few MJ is required for such high gain. With increasing α, the implosion laser energy required for generating the same size core increases, which leads to lowering Q_{max}, especially in the high-gain region. In the present case, the gain becomes $\sim 4/7$ in the high-gain region when α increases from 2 to 3. For high gain, therefore, low-isentrope implosion is also required.

In Fig. 5, we plotted a limiting gain curve evaluated by

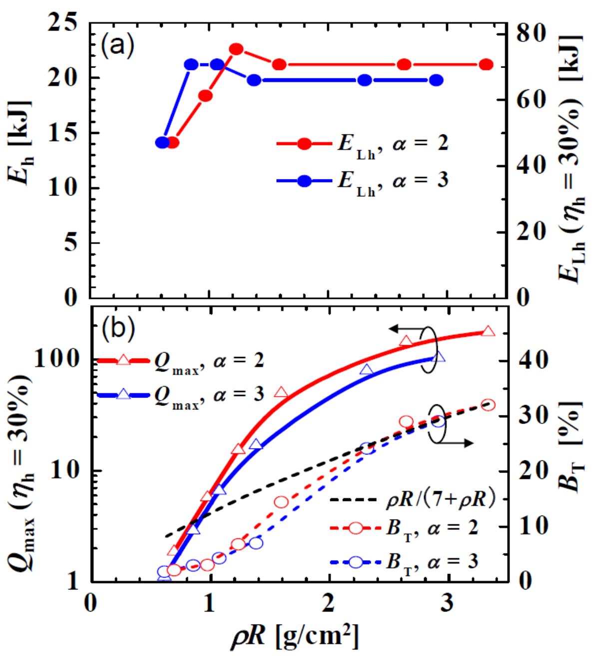

Fig. 4 Core-size dependences of (a) heating energy E_h (and the corresponding laser energy ($\eta_h = 30\,\%$)) required to achieve the maximum gain Q_{max} for each target and (b) the corresponding Q_{max} and the burn-up ratio B_T. B_T estimated using Eq. (1) is also plotted.

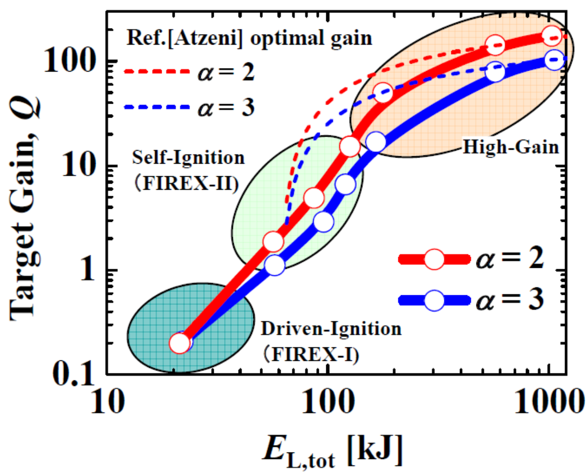

Fig. 5 Maximum gain Q_{max} as a function of total laser energy, $E_{L,tot} = E_{L,i} + E_{L,h}$. The red and blue solid curves represent simulation results for $\alpha = 2$ and 3 cores, respectively. The thin broken lines are the optimum gain curve evaluated in Ref. [2].

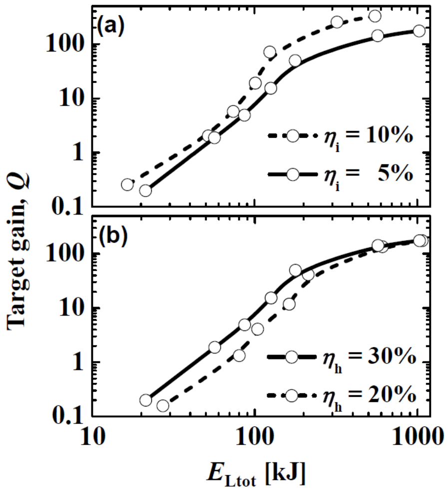

Fig. 6 Target gain dependence on coupling efficiencies between laser and core. (a) Dependence on the coupling of implosion laser η_i where η_h = 30 % and, (b) dependence on the coupling of heating laser η_h where η_i = 5 %. (α = 2 cores).

Atzeni [2],

$$G^* = 18000\eta_i^{7/6}\eta_h^{0.24}\left(\frac{E_{L,tot}\mathrm{MJ}}{\alpha^3}\right)^{7/18} \times (E_{L,tot}\mathrm{MJ})^{0.018}, \quad (2)$$

where the ignition energy was evaluated on the basis of numerical simulations for a sufficiently large core and the burn-up ratio was evaluated using Eq. (1). Thus, the limiting gain curve is not appropriate for a small core region, such as the driven ignition and self-ignition regions, although it agrees well with the present simulation results in the high-gain region.

In the above discussion, we assumed η_i = 5 % and η_h = 30 % for gain estimation. However, these values have not been proved in practice. The gain sensitivities to the coupling efficiencies were checked.

In Fig. 6 (a), Q_{max} evaluated for α = 2 is plotted as a function of $E_{L,tot}$ for η_i = 5 and 10 %, where the heating coupling is fixed as η_h = 30 %. If η_i doubles, half the implosion laser energy is needed to generate the same core (or the core volume becomes twice as large with the same implosion laser energy), which enhances the target gain. In the low-gain region, where $E_{L,i} \sim E_{L,h}$, gain enhancement resulting from an increase in η_i is not remarkable. In contrast, in the high-gain region, where $E_{L,i} \gg E_{L,h}$, the gain enhancement is significant. For instance, for $E_{L,tot} \sim 600$ kJ, Q_{max} = 143 for η_i = 5 % and Q_{max} = 327 for η_i = 10 %.

In Fig. 6 (b), Q_{max}, evaluated for α = 2 by assuming η_h = 20 and 30 %, is plotted as a function of $E_{L,tot}$, where the implosion coupling is fixed as η_i = 5 %. In the low-gain region ($E_{L,tot}$ < 200 kJ) where $E_{L,i} \sim E_{L,h}$, the reduction in Q_{max} due to decrease in η_h is clear. In the high-gain region, where $E_{L,i} \gg E_{L,h}$, it slightly affects gain performance, though the reduction in η_h increases the heating laser energy (η_h = 20 → 30 %, $E_{L,h}$ = 70 → 100 kJ).

3.3 Heating pulse dependence in high-gain target

To achieve the high gain required for a fusion reactor (Q > 100), the required heating energy is $E_h \sim 21$ kJ (shown in Fig. 4), which corresponds to laser energy of $E_{L,h}$ = 70 kJ (η_h = 30 %). The above gain estimation is based on the simulations assuming r_h = 15 µm, ρL_h = 1 g/cm^2, and τ_h =10 ps. The heating depth is determined by the generated fast electron temperature. If the fast electron beam and the heating laser have the same spot and duration, the beam and laser intensities (I_h and $I_{L,h}$) are 3×10^{20} and 1×10^{21} W/cm^2, respectively. The effective temperature of fast electrons generated by a relativistic intense laser is generally evaluated using simple scaling [16];

$$T_h = 0.511\,(\gamma_{eo} - 1)\ \ [\mathrm{MeV}], \quad (3)$$

where γ_{eo} is the electron relativistic factor in the laser field ($\gamma_{eo} = \sqrt{1 + I_{L,h}\lambda_{L,h}^2/1.37 \times 10^{18}}$, $\lambda_{L,h}$ is the laser wavelength [µm]). The averaged range $\rho\lambda_h$ of fast electrons having temperature T_h is approximated by [15]

$$\rho\lambda_h \approx 0.6T_h\ [\mathrm{g/cm^2}]. \quad (4)$$

Using these relations, the heating depth of fast electrons, generated by the heating laser is

$$\rho L_h \approx 0.3\left(\sqrt{1 + \frac{I_{L,h}\lambda_{L,h}^2}{1.37 \times 10^{18}}} - 1\right)\ [\mathrm{g/cm^2}]. \quad (5)$$

For $I_{L,h} = 1 \times 10^{21}$ W/cm^2, the heating depth evaluated using Eq. (5) is 8.8 g/cm^2, which is much larger than the value assumed above and also the optimum depth for ignition (~1.2 g/cm^2 [2]). Thus, if the fast electrons have the temperature scaled by Eq. (3), the laser intensity should be lower to shorten the fast electron range.

Eq. (3) provides simple ponderomotive scaling for laser–plasma interaction (LPI) at the critical density. In FIREX, and the subsequent DEMO and commercial reactors, the heating pulse duration is 10 ps or longer. For such long-pulse intense lasers, the low-density pre-plasma on the cone inner surface is pushed by strong ponderomotive force, and the density profile steepens in an early stage of the main pulse irradiation [17, 18]. Then, the heating pulse directly interacts with a dense plasma. On the basis of 2D collisional PIC simulations, Sentoku *et al.* [19] showed that, in this situation, T_h is drastically decreased without reducing the coupling efficiency from laser to fast electrons, and derived a new scaling for T_h;

$$T_h = 0.511\,[\gamma_{eo} - 1]\,\sqrt{\frac{\gamma_{eo}n_c}{n_{e,LPI}}}\ [\mathrm{MeV}], \quad (6)$$

where $n_{e,LPI}$ is the electron number density at the LPI region. Using this scaling, T_h is reduced by $\sqrt{\gamma_{eo}n_c/n_{e,LPI}}$

after the density profile steepens. For instance, when the heating laser with $I_{L,h} = 1 \times 10^{21}$ W/cm^2 interacts directly with a solid Au cone ($Z = 50$), where the $n_{e,LPI} = 2930n_c$, the fast electron temperature is $T_h = 1.44$ MeV. The range of those electrons is $0.6T_h = 0.87$ g/cm^2, which is slightly shorter than the optimum value. One way to increase the heating depth is to use higher intensity lasers. Another is to use a low density material for generating fast electrons. By attaching a low density material, such as a foam Au [20], on the cone inner surface, we can control the fast electron temperature and the heating depth without changing laser intensity.

The realization possibility of heating pulse parameters assumed above has not been clarified. In laser-cone interaction, fast electrons are generated with a certain angular spread (e.g., an opening half-angle of 22.5 degrees (FWHM) is observed in cone experiments [4]). The heating spot size is therefore determined by the cone tip size, the angular spread of fast electrons, the cone tip size, and the distance between the cone tip and the edge of the dense core, if we neglect the pinch and divergence of electron beam during propagation. For heating pulse duration, Nakamura *et al.* [21] performed 2D PIC simulations for laser-cone interactions, and observed longer electron beam emission from the cone tip than the duration of the irradiated laser. This means that the core heating time is not determined solely by the duration of the heating laser. To evaluate the sensitivities of ignition conditions and gain performance to the heating pulse shape and the heating depth, we performed the simulations for the H2 core with $\alpha = 2$ by varying ρL_h, r_h, and τ_h.

Heating depth

When the energy of fast electron is so high, the range is longer than the optimum heating depth (1.2 g/cm^2 [2]). In this case, larger heating pulse intensity and energy are required than the optimum values. Figure 7 (a) shows a plot of the ρL_h dependences. The duration and spot size of the heating pulse are fixed at $\tau_h = 10$ ps and $r_h = 15$ µm, respectively. If the heating depth becomes larger than the optimum value, more energy is required for heating the additional region. Compared with the $\rho L_h = 1$ g/cm^2 case, I_h and E_h required for ignition and Q_{max} are slightly high for $\rho L_h = 2$ g/cm^2, and Q_{max} decreases a little. If ρL_h becomes three times longer, the I_h and E_h required for Q_{max} increase by 20 % and $Q_{max}(\eta_h = 30\,\%)$ decreases by only 3.6 %. On the other hand, if the heating depth becomes shorter than 1 g/cm^2, the size of heating region becomes smaller than the optimum value determined by the 3.52 MeV alpha-particle range. In addition, the portion of the heated region boundary facing the low density coronal plasma increases, which increases the energy loss due to expansion into the low density region. Thus, the increases in I_h and E_h required for ignition and the decrease in Q_{max} with decreasing ρL_h are remarkable compared with deeper core heating.

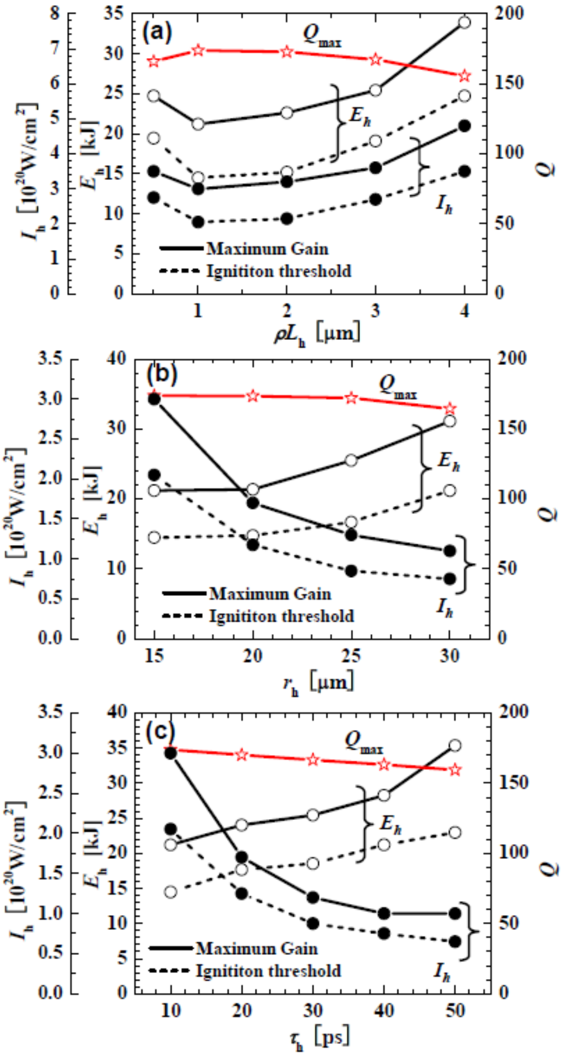

Fig. 7 Heating pulse dependence of ignition and gain performance for the H2 core ($\alpha = 2$). Dependence on (a) depth ρL_h, (b) spot size r_h, and (c) duration τ_h.

Spot radius

The pulse intensity is proportional to r_h^{-2}, therefore, larger r_h leads to intensity reductions. However, the heating region becomes larger than optimum, and the energy loss due to expansion increases, so the required heating energy might increase. In Fig. 7 (b), we plotted I_h and E_h, required for ignition (broken lines) and for Q_{max} (solid lines), and also plotted Q_{max} ($\eta_h = 30\,\%$) as a function of r_h, where τ_h and ρL_h are fixed at 10 ps and 1.0 g/cm^2. With increasing r_h, the heating pulse intensities required both for ignition and Q_{max} decrease, although E_h increases slightly; when r_h increases from 15 to 25 µm, I_h required for Q_{max} becomes less than half (1.3×10^{20} W/cm^2) and E_h increases by only 20 %. In the high-gain region, $E_{L,h} \ll E_{L,i}$ and the burn-up ratio does not change much. Thus, the value of Q_{max} depends slightly on r_h in the region of 15 to 25 µm. For a larger spot ($r_h > 25$ µm), the reduction in I_h is saturated, and the enhancement in E_h is remarkable. Thus, the spot radius is required to be smaller than 25 μm.

Pulse duration

Lengthening the pulse duration also reduces the heating pulse intensity. However, defects resulting from expansion of the heated region (i.e., the energy loss due to expansion and the decrease in density) become large, which increases the E_h requirement. In Fig. 7 (c), we plotted I_h and E_h, required for ignition (broken lines) and for Q_{max} (solid lines), and also plotted Q_{max} (η_h = 30 %) as a function of τ_h, where r_h = 15 μm and ρL_h = 1.0 g/cm^2. An increase in τ_h decreases the heating pulse intensities I_h required for ignition and Q_{max}, and requires a slightly larger E_h. In addition, the time taken to reach explosive burning becomes long. During this transition time, the fuel gradually disassembles and its size (ρR) becomes smaller, which results in a decrease in B_T. The reduction in Q_{max} with increasing τ_h, thus, is mainly due to the core disassembly. The reduction in heating pulse intensity with increasing τ_h is saturated when τ_h > 30 ps, which results in monotonic increase of heating energy. Thus, the pulse duration should be shorter than 30 ps.

The values of I_h and E_h required for ignition are sensitive to heating pulse parameters, as shown in Fig. 7. Those sensitivities are almost the same as the previous ones [5]. The values of I_h and E_h required for Q_{max} are larger than those for ignition by 27 to 54 %. The value of Q_{max} is not as sensitive to heating pulse parameters because $E_{L,i} \gg E_{L,h}$.

We performed simulations for the H2 core by assuming a large spot and a long duration, such as r_h = 25 μm and τ_h = 30 ps, to reduce the beam intensity. The heating depth is assumed to be ρL_h = 2.0 g/cm^2 We obtained that the required heating pulse intensity and energy are 5×10^{19} W/cm^2 and 30 kJ for ignition, and 7×10^{19} W/cm^2 and 41 kJ for Q_{max}. When η_h = 30 % (20 %), the corresponding heating laser energy is 98 kJ (147 kJ) for ignition and 137 kJ (206 kJ) for Q_{max} = 155 (146)—twice that of the optimum heating case (r_h = 15 μm, τ_h = 10 ps, and ρL_h = 1.0 g/cm^2). These results show that in a practical case, a heating laser of 150 to 200 kJ is required for successful burning in FI.

3.4 Foam effects

In the near future, foam targets are planned for use in DT experiments (such as FIREX-I [5]) and also in the reactor design of KOYO-FAST [6]. In FIREX-I, Resorcinol Formaldehyde–Phloroglucinolcarboxylic acid and Formaldehyde, $(C_8H_6O_2)_2$-$(C_7H_5O_4)$ (RF-PF) foam is one candidate for foam material [22]. A foam density of 100 mg/cc and a thickness of 7 μm have been achieved, and further development is ongoing. Using a foam target, the middle-Z ions such as carbon and oxygen are mixed in the compressed core. These ions enhance radiation loss from the heated region, which will make the ignition conditions more severe and reduce burn performance.

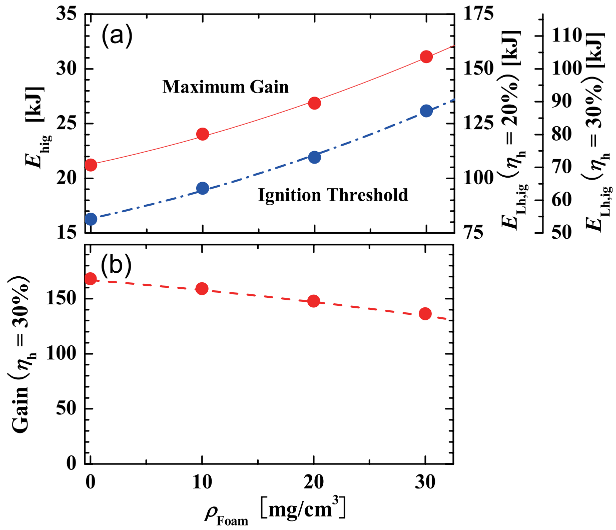

Fig. 8 Influences of RF-PF foam on ignition and gain of the H2 core (α = 2). (a) E_h required for ignition (blue) and Q_{max} (red) and (b) Q_{max} (η_i = 5 % and η_h = 30 % assumed) as a function of foam density at the solid state ρ_{foam}. The right axes in (a) show the corresponding heating laser energies.

To evaluate the allowable density of the RF-PF foam, we performed simulations for the H2 core (α = 2) by varying the foam density at the solid state from 0 to 30 mg/cc. The heating pulse parameters are fixed at γ_h = 15 μm, τ_h = 10 ps, and ρL_h = 1.0 g/cm^2. Figure 8 shows (a) heating energy required for ignition and Q_{max}, and (b) Q_{max} (where η_i = 5 % and η_h = 30 % are assumed) as a function of foam density ρ_{foam} at the solid state. For ρ_{foam} = 30 mg/cm^3, E_h required for ignition (for Q_{max}) increases by 60 % (47 %) compared with pure DT, and Q_{max} is reduced by 20 %. This means that the influence of foam is more significant on the ignition requirement than gain performance, and the allowance of foam density is determined by the limitation of the heating laser. If the increase in $E_{L,h}$ resulting from the foam material is limited within 30 %, the foam density should be smaller than 20 mg/cm^3, and maximum gain is reduced by 10 %.

4. Conclusions

On the basis of parametric 2D burn simulations for highly compressed DT cores (ρ = 300 g/cm^3), the ignition requirement and gain performance were evaluated for cores of various sizes (ignition-experiment-grade to reactor-grade); these results were compared with previous studies. For achieving sufficiently high burn-up ratio (more than 20 %), a core size of ρR > 2.0 g/cm^2 is required. For such large cores, the ignition requirement and the gain curve obtained in the present study agree well with previous evaluations [2]. The target gain is sensitive to η_i and α in the high-gain region, and is sensitive to η_h in the ignition experiment region.

We also examined the sensitivities of the heating pulse parameters to ignition and burn performance, and the influence of foam material for a reactor-grade core. For an optimum pulse, minimizing heating energy for a given heating depth, i.e., $\tau_h = 10$ ps and $r_h = 15\,\mu$m, requires a very high intense pulse (more than 3×10^{20} W/cm^2) for successful burning. If the heating laser has the same spot and radius as the heating pulse, a laser intensity $> 10^{21}$ W/cm^2 is required ($\eta_h = 30\,\%$). In accordance with the new temperature scaling for fast electrons generated by long pulse heating laser, such a high intensity laser is favor in the generation of fast electron having a suitable stopping range for efficient core heating. With increasing heating pulse duration and spot radius, the required heating energy becomes high. For $\tau_h = 30$ ps and $r_h = 25\,\mu$m, the heating energy doubles; when $\eta_h = 30\,\%$, the heating laser energy required for maximum gain is 137 kJ.

For a reactor-grade core, the influence of foam material on ignition requirements is more remarkable than that on gain performance. To limit the increase in $E_{L,h}$ required for Q_{max} within 30 %, the foam density is limited to 20 mg/cm^3.

The crucial issues for successful burning in fast ignition are high-convergence implosion and efficient core heating, which have not been discussed in detail in the present paper. The implosion dynamics of cone-guided targets (e.g., the influence of additional non-uniformity due to cone attachment on implosion performance and on formation of a high-density, low-isentrope and large-ρR core) and the detailed physics of heating process (e.g., fast electron generation and its energy transport into the dense core) have not been clarified. To understand each important physics mechanisms, detailed simulations (e.g., implosion of cone-guided targets [23], fast heating simulations [8, 9, 19, 24]) are ongoing. For detailed and self-consistent research, an integrated simulation study has begun [25], which includes implosion dynamics, fast electron generation at the relativistic laser-plasma interaction, fast electron energy transport into the dense core, and fusion burning. Integrated experiments using more powerful lasers will start soon (e.g., FIREX experiments at ILE, Osaka university [14] and OMEGA-EP experiments at LLE, Rochester university [26] will start within one or two years, and the EU group has proposed the HiPER project [27]). We expect these numerical and experimental studies to lead to detailed understanding of fast ignition physics and quantitatively accurate modeling for dense core profile and heating properties, which will modify, but not alter, the basic findings of the present paper.

Acknowledgments

This work was supported by MEXT, the Grant-in-Aid for Creative Scientific Research (15GS0214) and partially by the Grant-in-Aid for Encouragement of Young Scientists (B) (17760666). We are grateful for the support of the computer room of ILE and the cybermedia center at Osaka University.

[1] M. Tabak *et al.*, Phys. Plasmas **1**, 1626 (1994).
[2] S. Atzeni, Phys. Plasmas **6**, 3316 (1999).
[3] M. Tabak and D. Callahan, Nucl. Instrum. Methods. A **544**, 48 (2005).
[4] R. Kodama *et al.*, Nature **412**, 798 (2001); R. Kodama *et al.*, Nature **418**, 933 (2002).
[5] H. Azechi and the FIREX Project, Plasma Phys. Control. Fusion **48**, B267 (2006).
[6] K. Tomabechi *et al.*, *Conceptual Design of Fast Ignition Power Plant* (Institute of Laser Engineering, Osaka University and IFE Forum, 2006).
[7] T. Johzaki *et al.*, *Proc. International Conference on Inertial Fusion Sciences and Applications*, 2003 (IFSA2003), Monterey, CA, 2003 (American Nuclear Society, 2004) p.474.
[8] C.D. Levermore and G.C. Pomraning, Astrophys. J. **248**, 116 (1981).
[9] T. Johzaki *et al.*, Nucl. Fusion **39**, 753 (1999).
[10] T. Johzaki *et al.*, Laser Part. Beams **15**, 259 (1997).
[11] S.A. Slutz and R.A. Vesey, Phys. Plasmas **12**, 062702 (2005); S.A. Slutz *et al.*, Phys. Plasmas **11**, 3483 (2004).
[12] T. Johzaki *et al.*, J. Phys. IV France **133**, 385 (2006).
[13] T. Yokota, Y. Nakao, T. Johzaki and K. Mima, Phys. Plasmas **13**, 022702 (2006).
[14] K. Mima, Annual Progress Rep. 2001 (Institute of Laser Engineering, Osaka University, 2001) p.1.
[15] S. Atzeni and M. Tabak, Plasma Phys. Control. Fusion **47**, B769 (2005).
[16] S.C. Wilks *et al.*, Phys. Rev. Lett. **69**, 1383 (1993).
[17] H. Sakagami *et al.*, Europhysics conference abstracts, 30I, (33rd European Physical Society Conference on Plasma Physics Contributed Papers), European Physical Society, (CD-ROM;ISBN2-914771-40-1), P1.013 December, 2006; also available at http://eps2006.frascati.enea.it/papers/pdf/P1_013.pdf.
[18] T. Johzaki *et al.*, Europhysics conference abstracts, 30I, (33rd European Physical Society Conference on Plasma Physics Contributed Papers), European Physical Society, (CD-ROM;ISBN2-914771-40-1), P1.016 December, 2006; also available at http://eps2006.frascati.enea.it/papers/pdf/P1_016.pdf.
[19] Y. Sentoku *et al.*, "*Full scale PIC simulation of cone-guided fast ignition*," presented at the 9th international fast ignition workshop, Nov. 2006, Cambridge, MT, USA.
[20] A.L. Lei *et al.*, Phys. Rev. Lett. **96**, 255006 (2006).
[21] T. Nakamura *et al.*, J. Phys. IV France **133**, 401 (2006).
[22] F. Ito *et al.*, Jpn. J. App. Phys. **45**, L335 (2006).
[23] H. Nagatomo *et al.*, J. Phys. IV France **B133B**, 397 (2006); Phys. Plasmas **14**, 056303 (2007).
[24] J.J. Honrubia and J. Meyer-ter-Vehn, Nucl. Fusion **46**, L25 (2006).
[25] H. Sakagami and K. Mima, *Proc. International Conference on Inertial Fusion Sciences and Applications 2001* (IFSA2001), Kyoto Japan, 2001 (Elsevier, Paris, 2002) p.380; T. Johzaki *et al.*, J. Plasma Fusion Res. Series **6**, 341 (2004); H. Sakagami *et al.*, Laser Part. Beams **24**, 191 (2006).
[26] C. Stoeckl *et al.*, Fusion Sci., Technol. **49**, 374 (2006).
[27] M. Dunne, Nature Phys. **2**, 2 (2006).